Experimental investigation of immiscible liquids flow in a T-shaped microchannel

Anna Yagodnitsyna*, Alexander Kovalev, Artur Bilsky

Kutateladze Institute of Thermophysics, Novosibirsk, Russian Federation
Novosibirsk State University, Novosibirsk, Russian Federation
*corresponding author: yagodnitsinaaa@gmail.com

Abstract Flow regime visualization for immiscible liquid-liquid flow in a T-shaped microchannel with rectangular cross-section was done. For three sets of immiscible liquids, kerosene – water, paraffin oil – water and castor oil – paraffin oil flow patterns in a wide range of Weber numbers were obtained. Following typical flow patterns were observed: parallel flow, slug flow, plug flow, dispersed (droplet) flow and rivulet flow. The main difference of the experiment is in wettability of channel walls by all liquids used. As the consequence of that rivulet flow existence and absence of annular flow were observed. At high Weber numbers new flow pattern called serpentine flow was found. It was shown that flow pattern maps based on Weber numbers for different liquid sets does not match well. Weber number multiplied by liquid viscosity proposed as universality parameter for universal flow map. For plug flow regime plug length, velocity and flow circulation inside plug were evaluated.
Keywords: liquid-liquid flow, microchannel, micro-PIV, flow pattern map

1 Introduction

Immiscible liquid-liquid flows in microchannels have wide area of applications such as emulsion production [1], nitration [2] and extraction processes [3] and other biochemical applications [4]. Microchannel devices provide higher heat- and mass- transfer rates and possibility to organize fast, continuous and safe chemical reactions. In addition energy cost to create one unit of interfacial area between two liquids in microchannel devices is less than in other alternative processes [5]. There are also promising devices for biological analysis based on droplet microfluidics. The efficiency of such systems could be higher than of traditional devices by an order of magnitude [6]. One of the key components of microfluidic devices are systems for droplet generation, transportation and sorting.

Obviously, the efficiency of certain technological process is defined by regimes of two-component liquid flows in microchannel. For immiscible liquids plug flow is typical and optimal for chemical reactions. In this regime heat- and mass- transfer ensues from convection inside plugs ([7-9]) and diffusion along contact interface. In such a case mass transfer is intensified due to liquid circulation inside plugs. There are a number of parameters which influence on plug flow stability and formation such as liquid viscosity, velocity, phase ratio and so on. Tice et al. [10] analyzed these factors for water plugs formation in carrying fluid in rectangular micromixer.

Kashid and Agar [5] carried out experiments in Y-shaped capillary microreactors and defined region of plug flow existence for different volume rate ratios and channel diameters. To describe plug characteristics they used plug volume and surface to volume ratio of plugs. With increase of flow velocity volume and size of plugs increases which is also confirmed by [11]. Plug velocity is proportional to average flow velocity and proportionality factor depends on flow regime [12].

Pressure drop is also an important parameter in microreactor design and optimization. Kashid and Agar [5] studied pressure drop in plug flow. They took into account liquid film on the walls of round channel and showed a good agreement between experimental and theoretical data. Later Jovanovich et al. [11] proposed analytical model with account of movement of liquid film and found such consideration not to make significant contribution to result.

Liquid-liquid flows are characterized not only by plug flow. In different flow rates the following regimes can occur: droplet flow, slug flow, parallel and annular flow. Phase interaction and therefore flow regimes are defined by interfacial tension, inertia and viscous forces. Comparative impact of these forces can be expressed in terms of Reynolds number, Weber number and Capillary number. Zhao et al. [13] studied flow regimes in T-shaped microchannel with demonized water and kerosene as working fluids. When

constructing the flow pattern map they used Weber numbers of both phases. Regions of stable regimes depended on flow velocity and volume rate ratio. Three flow regime areas have been defined on the flow map: interfacial tension force domination, area with interfacial tension and inertia forces comparable, and area with inertia forces dominating. Foroughi and Kawaji [14] constructed similar flow pattern map for water and oil using non dimensional parameters Re, Ca and We and divided it into five area with different flow regimes. Kashid and Kiwi-Minsker [15] used non dimensional parameter Laplace number La = Re/Ca of carrying fluid in dependence of parameter Re•d/ε of disperse fluid, where ε – is volume ratio of disperse fluid. They defined three zones depending on ratio between capillary and inertia forces. In such flow map flow regime is defined by disperse phase velocity only. This statement can also be used for gas-liquid flows in microchannels [16] and applicable for cases when one of the liquids is dispersed and does not wet channel walls. Another one interesting consideration for flow map construction is described in [17], where authors used dimensional analysis for gas-liquid flows. Resulting complex $Re^{0.2}We^{0.4}$ gave a good generalization of experimental results. But usage of this criterion for data from literature does not give satisfactory results.
The main difficulty at the present moment is lack of scientific data generalization allowing explicitly predict flow regime and parameters of liquid-liquid two phase flow in microchannels. In particular there is no abundant investigation of influence of such parameters as density, viscosity and interfacial tension. Study of contact angle influence of flow regime is also absent. Moreover in majority of works one of liquids does not wet channel walls which make it dispersed phase. On the one hand it allows to drawn an analogy with gas-liquid flows. On the other hand cases when both liquids wet channel walls remain unexplored.
The present work considers immiscible liquid-liquid flows in rectangular microchannels. Experiments were carried out for several sets of liquids with different properties (viscosity, density, interfacial tension, contact angle). Flow visualization, velocity and length of the plugs are presented. Data are summarized by flow pattern maps.

2 Experimental setup

We used water, kerosene, paraffin oil and castor oil as working fluids. Not all physical parameters of organic liquids are provided by manufacturer standards and sometimes have wide range of deviation. Therefore density and viscosity of working fluids have been measured directly. For viscosity measurement capillary viscometer (for water and kerosene) and rotation viscometer (for paraffin and castor oils) were used. Relative measurement error was 1% and 3%, respectively. Density was measured by weighting of known volume of liquid. Relative measurement error of density was 1%. Physical properties of used liquids are shown in Table 1.

Table. 1 Physical properties of liquids

Physical properties	**Kerosene**	**Water**	**Paraffin oil**	**Castor oil**
Density, kg/m^3	745	997	845	935
Viscosity, mPa•s	0.820	0.894	110	650
Interfacial tension, mN/m	45		48	14

T-shaped microchannel was manufactured by microLIQUID (Spain) from SU-8 material which has high wettability by all liquids used. We didn't do any special treatment of microchannel walls. Size of inlet channels was 200x200 um, size of outlet channel was 200x400 um. The length of inlet and outlet channels was 11.5 and 22.5 mm, respectively.

For flow regime visualization we used pco.1200 hs high speed camera and inverted Zeiss Axio Observer.Z1 microscope with 5x magnification objective. Shooting speed varied from 5 to 1000 Hz. Halogen lamp was used for flow illumination. Flow was organized by KDS Gemini 88 double syringe pump. Flow visualization was done in two different channel areas: T-zone and at the end of the channel, which is 56 channel hydraulic diameters far from T-zone. Experiments were carried out for wide range of Reynolds, Weber and Capillary numbers (Table 2).

Table 2 Experimental parameters

Parameters	**Water - Kerosene**	**Water - Paraffin oil**	**Paraffin oil - Castor oil**
Re	$0,02 < Re_w < 370$ $0,1 < Re_k < 250$	$0,02 < Re_w < 185$ $1,2 \cdot 10^{-4} < Re_p < 0,1$	$2,1 \cdot 10^{-5} < Re_p < 0,1$ $4 \cdot 10^{-6} < Re_c < 0,01$

We	$2{,}2\cdot10^{-8}<We_w<6{,}4$ $7{,}7\cdot10^{-7}<We_k<4{,}8$	$2{,}2\cdot10^{-8}<We_w<2{,}2$ $1{,}8\cdot10^{-8}<We_p<0{,}01$	$1{,}7\cdot10^{-9}<We_p<0{,}01$ $2\cdot10^{-9}<We_c<0{,}01$
Ca	$1{,}2\cdot10^{-6}<Ca_w<0{,}02$ $7{,}6\cdot10^{-6}<Ca_k<0{,}02$	$1{,}2\cdot10^{-6}<Ca_w<0{,}01$ $1{,}4\cdot10^{-4}<Ca_p<0{,}1$	$8\cdot10^{-5}<Ca_p<0{,}1$ $4{,}8\cdot10^{-4}<Ca_c<1{,}16$

Velocity field measurements inside water plugs were done by means of micro-PIV technique using POLIS PIV system. Water phase was seeded by 3 um fluorescent polystyrene particles. Flow was illuminated by double pulsed Nd:YAG laser. Particle images were captured using double exposure 4 Mpix CCD camera. Instantaneous velocity fields were calculated using iterative cross-correlation algorithm. Interrogation area was 128x128 pix with 50% overlapping.

3 Flow visualization results

For kerosene-water system flow regimes in wide range of Weber numbers were obtained including regimes with capillary and inertia forces domination. The main parameters influencing on flow regime are interfacial tension of liquids, channel wettability and ratio between liquid viscosities. Characteristic flow images for all regimes are shown on Fig.1. For these liquids the following flow regimes were noted: parallel flow including parallel flow with wavy interface, plug flow, slug flow, dispersed (droplet) flow and rivulet flow.

For small Weber numbers $10^{-6}<We_k<10^{-2}$ and $10^{-8}<We_w<10^{-3}$ for both liquids the flow with water plugs in kerosene occurs (Fig.1 b). When increasing water flow rate kerosene slugs in water carrying fluid is set up (Fig.1 d). Parallel flow exists in the range of Weber numbers $10^{-4}<We_k<1$ for kerosene and $10^{-4}<We_w<1$ for water. At high kerosene and low water flow rates droplet flow with small amount of polydisperse water droplets exists (Fig.1 c). At $We_w<10^{-5}$ periodical breakdown of two water droplets was observed with diameter ratio 2:3. Increasing water flow rate led to variable water droplet size, in such a case periodical droplet breakdown have not been observed. Rivulet flow exists in wide range of Weber numbers of both liquids (Fig.1 e). We observed both kerosene rivulet in water flow and water rivulet in kerosene flow; upon that rivulet flows are stationary. We consider rivulet flow to arise instead of annular flow because of high channel wettability by both liquids. At Weber numbers $We_k \sim We_w \sim 1$ new regime of parallel flow was discovered at which the shape of interfacial area has periodical wavy interface (Fig.1 f). It is important to notice that interface is stationary not only at the beginning of the channel but also at the end. This regime remains stationary up to $We_w<6$. With further increasing Weber numbers flow becomes nonstationary. Because of specific shape of interface we called it “serpentine flow”.

Found flow regimes were organized into flow map with Weber number at the axes (Fig. 2). Comparison with the work [13] in which kerosene and water flow in hydrophilic microchannel was investigated showed the following. In the case when one of the liquids does not wet channel walls plug flow exists only for one liquid and slug flow does not present. Moreover, instead of rivulet flow annular flow is observed and parallel flow exists in wider range of Weber numbers. The main reason of such disagreement can lie in different contact angles. This means that for different combination of liquids and channel materials different flow maps could be obtained. So, Weber number itself is not a resumptive parameter for flow maps and should be modified.

For paraffin oil – water system the following flow regimes were observed: plug flow (water in oil), parallel, dispersed flow (water droplets in water), slug flow (water in oil and oil in water) (Fig. 3). Paraffin oil in such combination of liquids has less contact angle with channel wall. Viscosity of paraffin oil is 120 times higher than of water. For small Weber numbers of paraffin oil $10^{-8}<We_p<10^{-4}$ and water $10^{-8}<We_w<10^{-6}$ water plugs in oil are observed. Increasing Weber number of paraffin oil while Weber number of water by an order of magnitude larger led to dispersed flow. Notably in some cases droplet coalescing and attachment to the channel walls was observed which resulted in droplet size growth. Parallel flow existed in a broad range of Weber numbers $10^{-8}<We_p<10^{-2}$ for paraffin oil and $10^{-6}<We_w<1$ for water.

Flow of paraffin oil and castor oil in microchannel is characterized by high viscosity of both liquids. Viscosity of castor oil is six times higher than of paraffin oil and two orders of magnitude higher than of

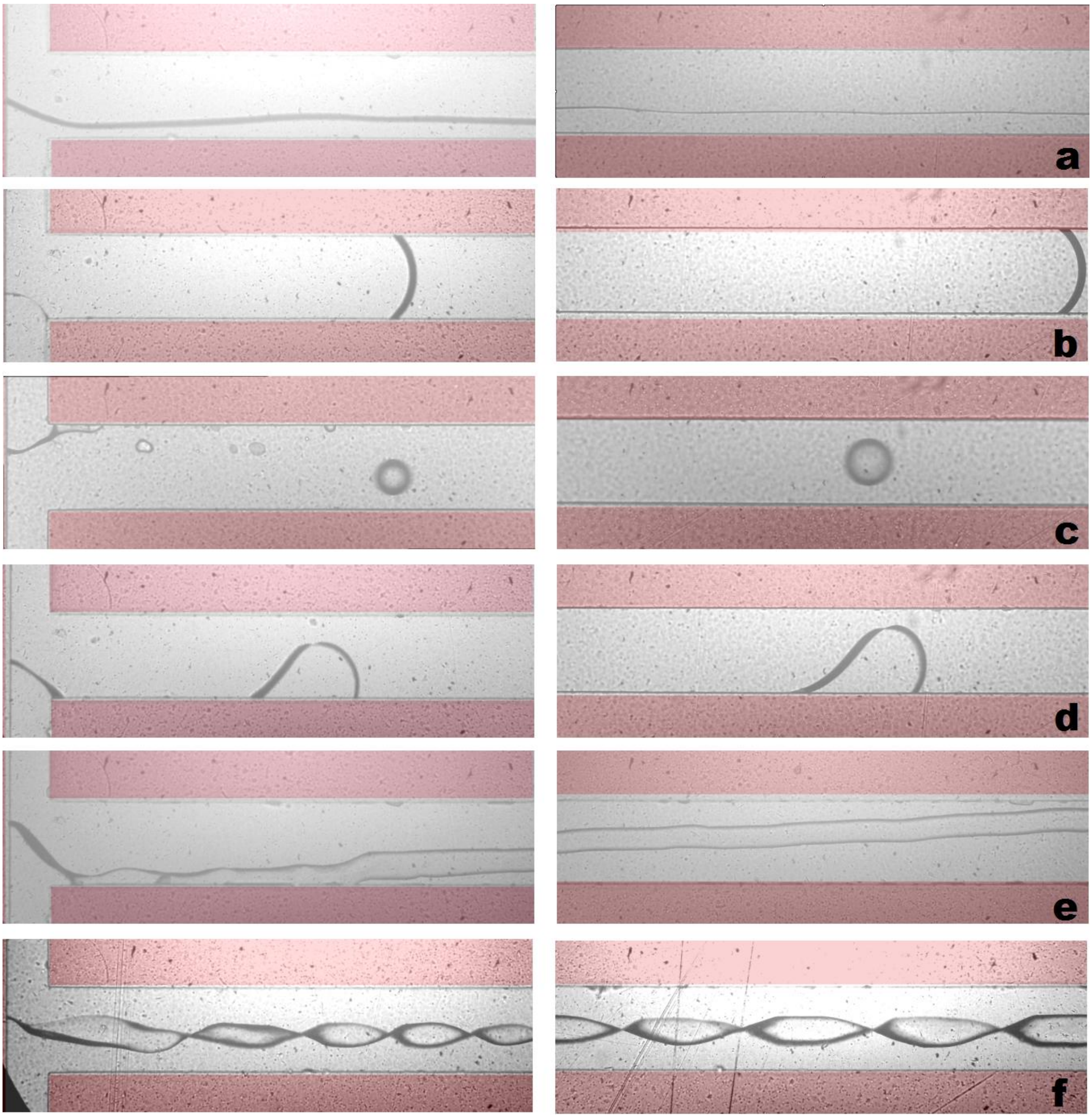

Fig. 1 Flow regime visualization of kerosene-water system at the beginning and end of the channel a) parallel flow $We_k = 1.1e\text{-}2$, $We_w = 2.4e\text{-}6$ b) plug flow $We_k = 1.1e\text{-}4$, $We_w = 4e\text{-}7$ c) droplet flow $We_k = 1.1$, $We_w = 2.6e\text{-}5$ d) slug flow $We_k = 1.1e\text{-}4$, $We_w = 0.43$ e) rivulet flow $We_k = 1.1e\text{-}2$, $We_w = 4.1$ f) serpentine flow $We_k = 3.1$, $We_w = 4.1$

kerosene and water. Because of maximum pressure limit of syringe pump we didn't achieve high Weber numbers in our experiments which were limited to 10^{-2}. Nevertheless we managed to record the following flow regimes: plug flow, slug flow, dispersed (droplet) flow, parallel flow and rivulet flow. The flow map is presented in Fig 2. One can readily see that regions of flow regime existence are shifted to lower Weber numbers while their relative position approximately coincides with other sets of liquids.

Comparison of three flow pattern maps for kerosene – water, paraffin oil – water and paraffin oil – castor oil showed that all of them are conformable. For all of three liquid combinations there are parallel flow, plug flow and slug flow. Their relative position remains similar for given selection of diagram axes. Nonrandom choice of axes arrangement implies that at certain combination of liquids one of them tends to be dispersive phase (vertical axe) while another one carrying phase (horizontal axe) even if both liquids wet channel walls very well. In particular this can cause droplet and slug flow to exist only for one phase. Notably these regimes are interfacial tension dominated. On the other hand for parallel and rivulet flow where interfacial tension does not play a key role none of the phases can be called dispersed. For example, in kerosene – water flow rivulet regime exists for both phases.

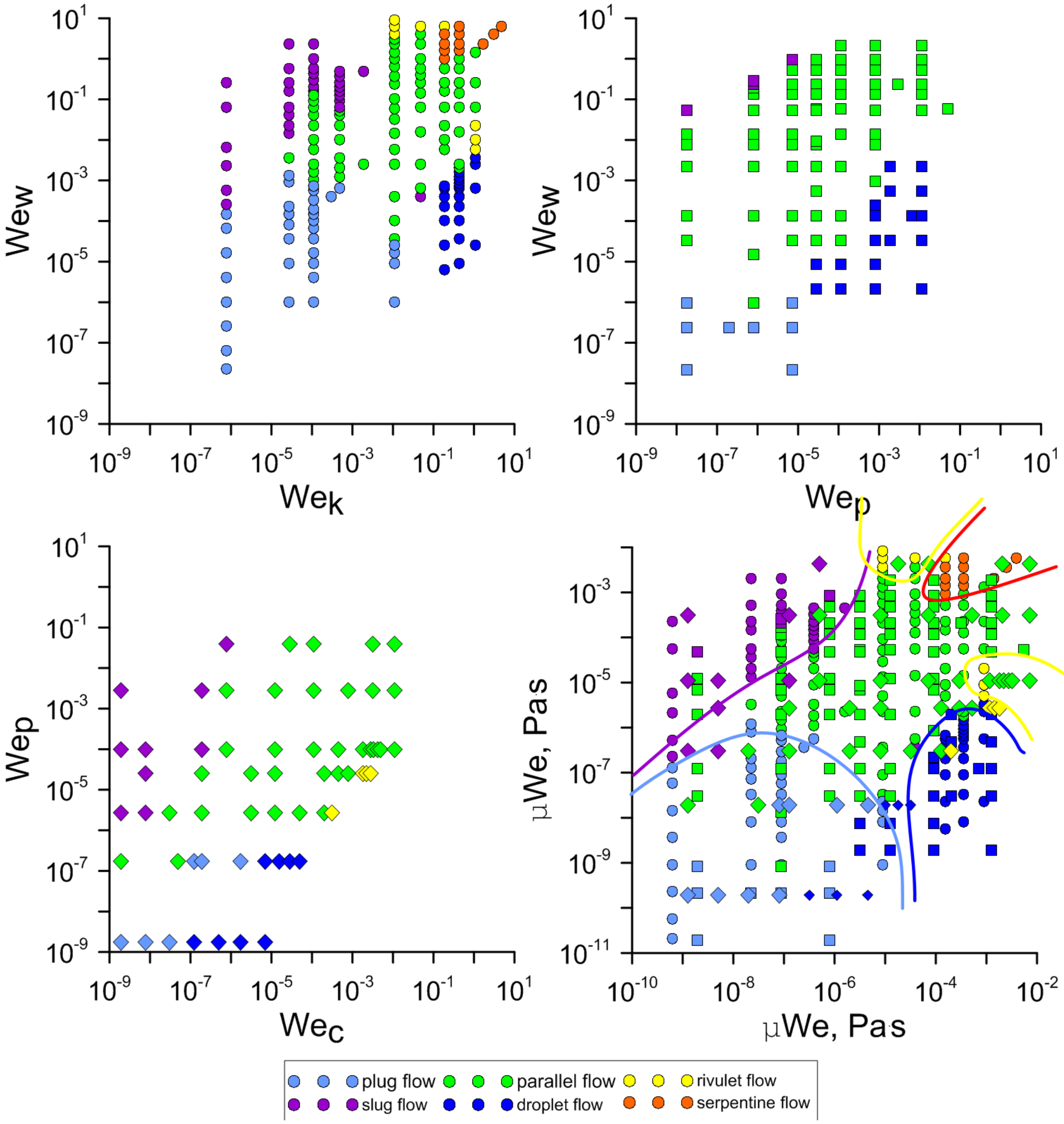

Fig. 2 Flow pattern maps for kerosene-water (top left), paraffin oil-water (top right), paraffin oil – castor oil (bottom left). Modified joint flow map for all liquid systems (bottom right).

One can easily see that boundaries of flow regime regions are shifted towards less Weber numbers for paraffin oil – water and paraffin oil – castor oil flows in comparison with kerosene- water flow. Thus flow pattern diagrams using Weber number as parameter are not comprehensive. In point of fact Weber number does not take into account such important parameters as liquid viscosities and channel wettability. By comparison flow pattern diagrams using superficial velocity does not consider parameters responsible for droplet and plug formation such as ratio between interfacial tension and inertia forces and also not universal.

In order to sum up obtained result we modified non-dimensional parameter to combine flow pattern maps. New parameter was received by multiplying liquid Weber number by its viscosity and has dimension Pa•s. General map for all three sets of liquids drawn in u•We coordinates is shown in Fig. 2. One can notice that regions of flow regimes for different sets of liquids coincide with each other. Therefore we can conclude that new parameter has more genericity than Weber number.

To examine genericity of proposed criterion we carried out comparison between flow pattern maps obtained in the present work with ones described in [13]. In Fig. 3 there are symbols corresponding to flow patterns obtained by Zhao et al. and flow regimes boundaries corresponding our experiments. Zhao et al. also used kerosene – water combination but in their case kerosene was dispersed phase. Keeping in mind the rule described we draw flow pattern map using the criterion with water (carrying fluid) on x-axes and kerosene on y-axes. One can see that for parallel, plug and droplet flow there is a good agreement. Slug flow did not exist in the work of Zhao et al., and droplets populations and annular flow exist in the area of rivulet and parallel (serpentine) flow for our case.

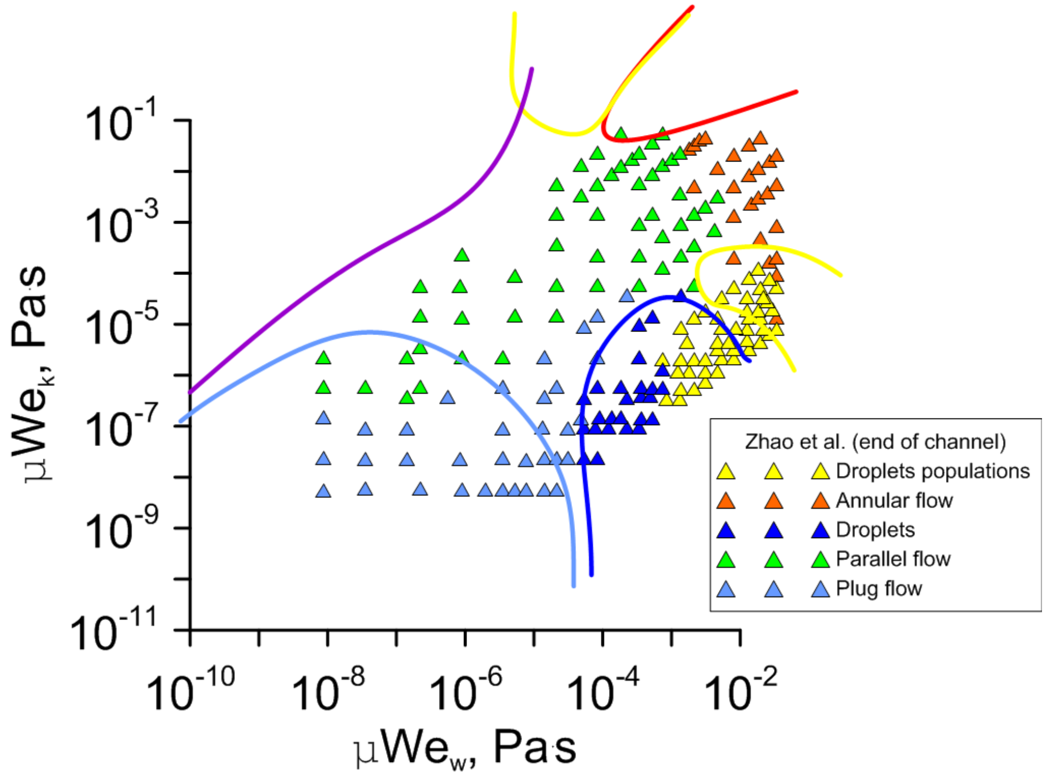

Fig. 3 Flow pattern maps for kerosene-water from [13] with modified parameter in comparison with flow regime boundaries

4 Hydrodynamic properties of plug flow

Plug flow in microchannels is of interest because it is most frequently used in different technical application (emulsion production, nitration and extraction processes). All these applications require experimental information describing hydrodynamic properties of the flow. For example chemical reaction rate is defined by plug velocity, length and velocity circulation inside plugs. In the present work on the basis of flow visualization results and velocity field measurement inside plugs by means of micro-PIV technique the following results characterized plug flow were obtained. All results are presented for kerosene – water flow.

In Fig.4 (left) a plot of plug length in dependence of total flow rate of both liquids is presented. Total flow rate was varied by keeping constant kerosene flow rate (24 ul/min) and varying water flow rate. In such situation plug length increases almost linear with total flow rate increase. In reverse situation when total flow rate increased due to kerosene flow rate increase plug length decreased [5, 13]. It is important to notice that length of plugs in the same regime varied in the range of 10% from average value. Plug velocity was always higher than bulk velocity in the channel (Fig.4 right). It means the presence of kerosene rivulets in the corners of the channel moving with less velocity than plug. Velocity values approximation gave dependence $U_{plug} = 1.21*U_{bulk}$ which is in a good agreement with results of Salim et al. [12], where coefficient of proportionality was equal to 1.28.

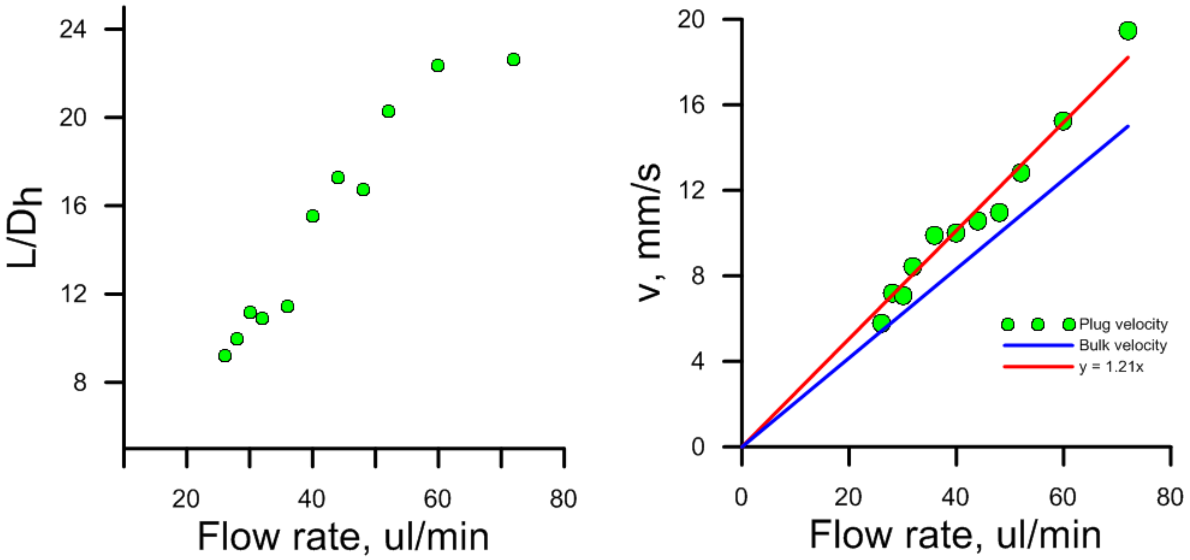

Fig. 4 Left: non-dimensional plug length in dependence of total flow rate. Right: plug velocity in dependence of total flow rate

Velocity field measurements in water plugs are done in the area of plug formation and at the end of the channel. Fig.5 illustrates instantaneous velocity fields in central plane of the channel in different phases of water plug formation. One can see (Fig.5 b) that water plug covers almost entire channel diameter which lead to local velocity increase of carrying fluid in constriction area. High velocity of carrying fluid results in high shear rates nearby plug crest and high water phase velocity. This mechanism is probably pivotal in droplet formation and breakup in droplet flow regime.

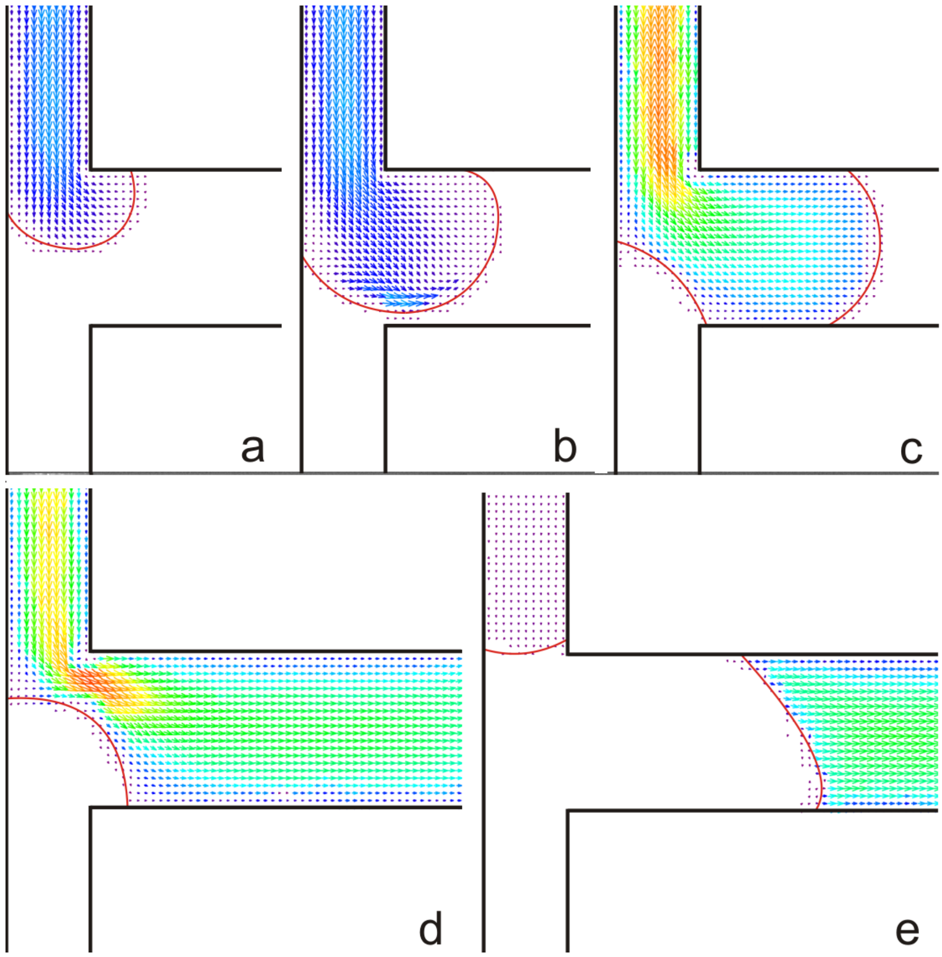

Fig. 5 Instantaneous velocity fields in central plane of the channel in different phases of water plug formation

In Fig. 6 velocity fields inside water plug at the end of the channel are presented. The maximum velocity is at the center of the plug and it decreases towards channel walls. In Fig.6 c the difference between instantaneous velocity field and plug velocity is shown. One can see circulation inside plug with different sign left and right from plug axe.

Based on measured velocity fields velocity circulation inside plugs was calculated for different flow rates. Velocity circulation was calculated using Green's theorem by integrating vorticity field over the surface bounded by curve shown in Fig.6 c. In all cases the boundaries of integrating area were chosen nearby channel walls and channel center. Calculated circulation was normalized by integrating surface area. This allowed avoiding dependence of circulation on the length of area. Circulation was calculated for two different curves shown in Fig 6 c (black and red curves). The difference in velocity circulations for two curves did not exceed 10%.

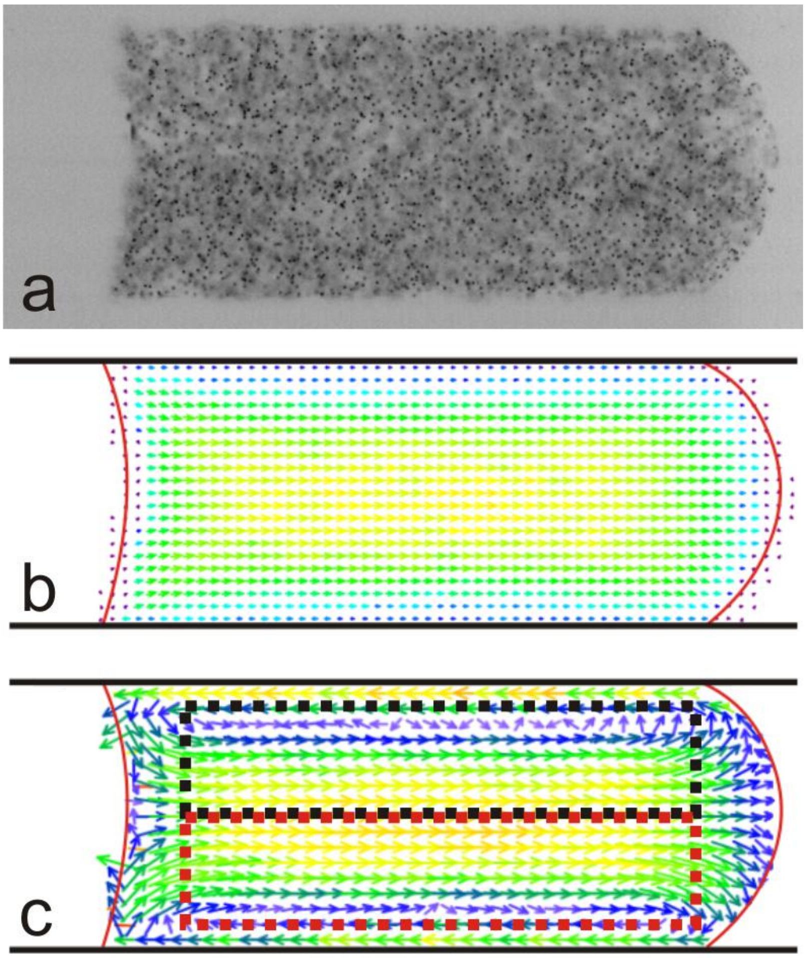

Fig. 6 a) Inverted tracer particle image b) Instantaneous velocity field in water plug at the end of the channel c) Velocity circulations inside the plug

Normalized velocity circulation values in different flow rates are presented in Fig.7. With plug velocity increase circulation also increases. It is obvious that circulation inside plugs defines intensity of convective mass transfer. In case of chemical reactions circulation is responsible for convective transfer of reagents. Thus circulation increase or, as follows from obtained result, plug velocity increase leads to decrease of reaction time. Nevertheless one should notice that reaction rate by microreactor unit length remains constant.

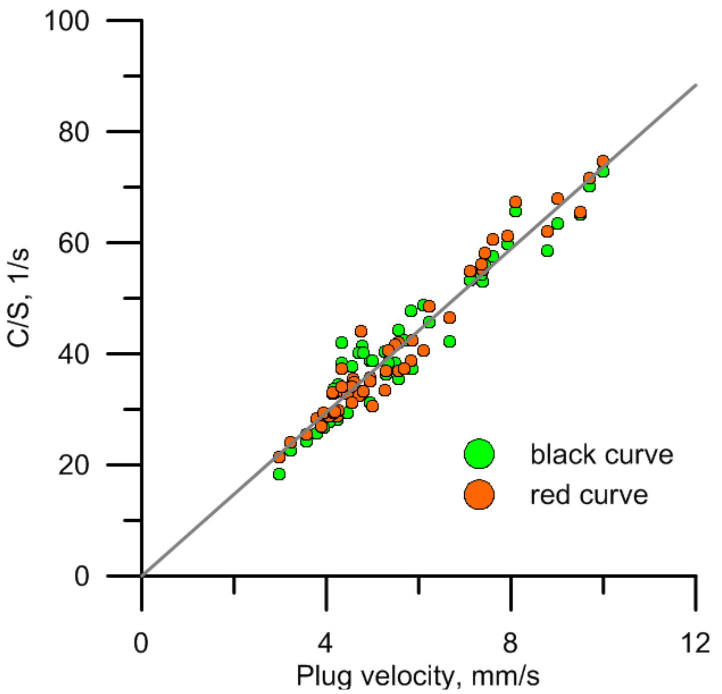

Fig. 7 Normalized circulation in water plugs versus plug velocity

5 Conclusion

Flow regime visualization for immiscible liquid-liquid flow in a T-shaped microchannel with rectangular cross-section was done. For three sets of immiscible liquids, kerosene – water, paraffin oil –water and castor oil – paraffin oil flow patterns in a wide range of Weber numbers were obtained. Flow regimes include those with interfacial tension and inertia forces domination. Fluids chosen have different physical properties. Kerosene and water have similar viscosity and density. Paraffin oil and water set give combination of high and low viscosity liquids. Paraffin oil and castor oil have different viscosities that higher by two order of magnitude than those for water and kerosene. Following typical flow patterns were observed: parallel flow, slug flow, plug flow, dispersed (droplet) flow and rivulet flow. The main difference of the experiment is in wettability of channel walls by all liquids used. As the consequence of that rivulet flow existence and absence of annular flow were observed. At high Weber numbers new flow pattern called serpentine flow was found. For this flow pattern liquid interface has a stationary wavy form up to the end of the channel.

For all of three liquid sets flow pattern maps based on Weber numbers were plotted. It was shown that relative positions of flow regimes on the map match together. Axes choice for flow map plotting is not random. Carrying fluid should be marked on horizontal axe while dispersed fluid on vertical axe. Resulted flow pattern maps cannot be generalized by simple overlapping. To combine all flow pattern maps into one we propose to use new parameter – Weber number multiplied by liquid viscosity. Flow map using this parameter gave a good agreement for different liquid sets.

Using visualization and velocity field measurement results the following results were obtained. It was shown what plug velocity is proportional to bulk velocity with coefficient of proportionality equal to 1.21. With increasing disperse flow rate plug length increases. Using velocity fields inside water plugs velocity circulation in different flow regimes was calculated. It was shown that circulation growths linearly with plug velocity.

Acknowledgments

The study was supported by RFBR, research projects NN. 14-08-00961 and 14-08-31502 mol_a.

References

[1] Christopher G.F. and Anna S.L. (2007) Microfluidic methods for generating continuous droplet streams, Journal of Physics D – Applied Physics, 40, R319-R336.

[2] Ducry L. and Roberge D.M. (2005) Controlled Autocatalytic Nitration of Phenol in a Microreactor, Angewandte Chemie International Edition, 44, 7972 –7975.

[3] Zhao Y., Chen G., Yuan Q. (2007) Liquid–liquid two-phase mass transfer in the T-junction microchannels AIChE J., 53, pp. 3042–3053.

[4] Benavides, J., Aguilar, O., Lapizco-Encinas, B.H., Rito-Palomares, M. (2008) Extraction and purification of bioproducts and nanoparticles using Aqueous Two-Phase Systems Strategies, Chemical Engineering & Technology, 31(6) pp. 838-845.

[5] Kashid, M.N., Agar, D.W. (2007) Hydrodynamics of liquid–liquid slug flow capillary microreactor: flow regimes, slug size and pressure drop, Chemical Engineering Journal 131, pp. 1–13.

[6] Tran T.M., Lan F., Thompson C. S. and Abate A. R (2013) From tubes to drops: droplet-based microfluidics for ultrahigh-throughput biology, J. Phys. D: Appl. Phys., 46, 11, 114004

[7] Burns, J.R., Ramshaw, C. (2001) The intensification of rapid reactions in multiphase systems using slug flow in capillaries. Lab on a Chip 1 , pp. 10–15.

[8] Dummann, G., Quittmann, U., Groschel, L., Agar, D.W., Worz, O., Morgenschweis, K. (2003) The capillary-microreactor: a new reactor concept for the intensification of heat and mass transfer in liquid–liquid reactions. Catalysis Today 79–80, pp. 433–439.

[9] Kashid, M.N., Gerlach, I., Goetz, S., Franzke, J., Acker, J.F., Platte, F., Agar, D.W., Turek,S. (2005) Internal circulation within the liquid slugs of a liquid–liquid slugflow capillary microreactor, Industrial and Engineering Chemistry Research 44, pp. 5003–5010.

[10] Tice, J.D., Lyon, A.D., Ismagilov, R.F. (2004) Effects of viscosity on droplet formation and mixing in microfluidic channels., Analytica Chimica Acta 507, pp. 73–77

[11] Jovanovich J., Zhou W., Rebrov E.V., Nijhuis T.A., Hessel V., Schouten J.C. (2011) Liquid–liquid slug flow: hydrodynamics and pressure drop. Chem.Eng.Sci. 66, pp. 42–54.

[12] Salim, A., Fourar M., Pironon J., Sausse J. (2008) Oil-water two-phase flow in microchannels: flow patterns and pressure drop measurements. Can.J.Chem.Eng. 86, pp. 978–988.

[13] Zhao Y., Chen G., Yuan Q. (2006) Liquid-liquid two-phase flow patterns in a rectangular microchannel, AIChE Journal, 52, Issue 12, pp. 4052–4060.

[14] Foroughi H., Kawaji M. (2011) Viscous oil–water flows in a microchannel initially saturated with oil: Flow patterns and pressure drop characteristics. International Journal of Multiphase Flow, 37, pp. 1147–1155

[15] Kashid M., Kiwi-Minsker L. (2011) Quantitative prediction of flow patterns in liquid–liquid flow in micro-capillaries, Chemical Engineering and Processig, 50, pp. 972– 978.

[16] Dessimoz A.L., Raspail P., Berguerand C., Kiwi-Minsker L. (2010) Quantitative criteria to define flow patterns in micro-capillaries, Chemical Engineering Journal 160 (3), pp. 882–890.

[17] Waelchli, S., Rudolf von Rohr, P. (2006) Two-phase flow characteristics in gas–liquid microreactors, International Journal of Multiphase Flow 32, pp. 791–806.